Physica Medica 33 (2017) 106–113

Contents lists available at ScienceDirect

Physica Medica

journal homepage: http://www.physicamedica.com

Original paper

A $^{13}C(d,n)$-based epithermal neutron source for Boron Neutron Capture Therapy

M.E. Capoulat *, A.J. Kreiner

Gerencia de Investigación y Aplicaciones, CNEA, Av. Gral. Paz 1499 (B1650KNA), San Martín, Buenos Aires, Argentina
CONICET, Av. Rivadavia 1917 (C1033AAJ), Buenos Aires, Argentina
Escuela de Ciencia y Tecnología, Universidad Nacional de San Martín, M. de Irigoyen 3100 (1650), San Martín, Buenos Aires, Argentina

ARTICLE INFO

Article history:
Received 26 September 2016
Received in Revised form 23 December 2016
Accepted 27 December 2016
Available online 31 December 2016

Keywords:
Accelerator-based BNCT
$^{13}C(D,N)^{14}N$ reaction
Monte-Carlo-simulations
Epithermal neutron sources
Brain tumor treatment

ABSTRACT

Purpose: Boron Neutron Capture Therapy (BNCT) requires neutron sources suitable for in-hospital siting. Low-energy particle accelerators working in conjunction with a neutron producing reaction are the most appropriate choice for this purpose. One of the possible nuclear reactions is $^{13}C(d,n)^{14}N$. The aim of this work is to evaluate the therapeutic capabilities of the neutron beam produced by this reaction, through a 30 mA beam of deuterons of 1.45 MeV.
Methods: A Beam Shaping Assembly design was computationally optimized. Depth dose profiles in a Snyder head phantom were simulated with the MCNP code for a number of BSA configurations. In order to optimize the treatment capabilities, the BSA configuration was determined as the one that allows maximizing both the tumor dose and the penetration depth while keeping doses to healthy tissues under the tolerance limits.
Results: Significant doses to tumor tissues were achieved up to ~6 cm in depth. Peak doses up to 57 Gy-Eq can be delivered in a fractionated scheme of 2 irradiations of approximately 1 h each. In a single 1 h irradiation, lower but still acceptable doses to tumor are also feasible.
Conclusions: Treatment capabilities obtained here are comparable to those achieved with other accelerator-based neutron sources, making of the $^{13}C(d,n)^{14}N$ reaction a realistic option for producing therapeutic neutron beams through a low-energy particle accelerator.

1. Introduction

1.1. Background

Boron Neutron Capture Therapy (BNCT) is a radiotherapy modality for the treatment of some types of locally invasive malignant tumors such as head and neck tumors and brain cancer, and other pathologies for which there are only palliative, low-effectiveness or mutilating treatments. The therapy consists in two steps. First and ideally, a highly tumor-selective drug containing ^{10}B is administered to the patient, which has a large capture cross-section for thermal neutrons. Then, the patient is irradiated with epithermal (0.5 eV < E < 10 keV) neutrons, which thermalize as they penetrate the tissues and are captured by ^{10}B predominantly present in tumor cells. Following the capture, high Linear Energy Transfer (LET) and short-range radiation (an alpha particle and a ^{7}Li ion) is produced, which damages the targeted cells without harming the surrounding tissue significantly.

One of the challenges in BNCT research has been the implementation of a sufficiently intense neutron source capable of producing a clean epithermal spectrum. Epithermal columns implemented on existing reactor facilities have been used to successfully treat patients with glioblastoma multiforme, intracraneal metastatic and subcutaneous melanoma, among others [1–6]. As an alternative to reactor facilities, accelerator-based (AB) neutron sources are under development at a number of institutions [7–15].

AB-neutron sources are in some aspects more advantageous than reactor-based ones. First, the neutron spectrum from certain nuclear reactions is much softer than the one coming from fission, which make it easier to generate the "ideal" epithermal spectrum, and hence to produce a neutron field of better therapeutic quality. Last but not least, because of their much lower cost and level of complexity, and mainly because they permit in-hospital siting.

Several neutron-producing reactions have been proposed for BNCT (Table 1). The $^{7}Li(p,n)^{7}Be$ reaction is the best option from the point of view of neutronics since it can provide an intense flux

* Corresponding author at: Gerencia de Investigación y Aplicaciones, CNEA, Av. Gral. Paz 1499 (B1650KNA), San Martín, Buenos Aires, Argentina.
E-mail address: capoulat@tandar.cnea.gov.ar (M.E. Capoulat).

http://dx.doi.org/10.1016/j.ejmp.2016.12.017
1120-1797/

Table 1
Characteristics of some neutron-producing reactions for BNCT and their target materials.

Reaction	Bombarding Energy [MeV]	Residual Radio-activity	Fraction [a] En < 1 MeV at 0°	Neutron Yield [n/mC]	Target melting point [°C]	Target thermal conductivity [W/m-K]	Reference
^{7}Li(p,n)^{7}Be[b]	2.3	Yes[d]	100%	5.8×10^{11}	181 °C	85	[17]
^{9}Be(p,n)^{9}B[b]	4.0	No[e]	50%	1.0×10^{12}	1287 °C	201	[18]
^{9}Be(d,n)^{10}B[c]	1.45	No	69%	1.6×10^{11}	1287 °C	201	[19]
^{13}C(d,n)^{14}N[b]	1.45	No	70%	1.9×10^{11}	3550 °C	230	[20]

[a] Percentage of yield at 0° for which the maximum neutron energy is less than 1 MeV.
[b] Thick target.
[c] 8 μm thick Be target.
[d] Decay of ^{7}Be: $T_{1/2}$ = 53.22 d. E_{γ} = 477.60 keV. Iγ = 10.44%.
[e] Very short lived ^{9}B with no gamma production.

of low energy (E_n < 1 MeV) neutrons. However, ^{7}Li is poorly suited as a high-power target, making its implementation for BNCT quite difficult (though not impossible). Moreover, the production of radioactive ^{7}Be ($T_{1/2}$ = 53 d) is a non-negligible complication to deal with in a hospital environment. In this context, neutron-producing reactions based on ^{9}Be or ^{13}C come up as an alternative. Both carbon and beryllium have far better thermal and chemical properties than metallic Li, and also, none of the involved nuclear reactions produce residual radioactivity. In the case of ^{9}Be(d,n)^{10}B and ^{13}C(d,n)^{14}N reactions, there is an additional advantage over ^{9}Be(p,n)^{9}B. Being endothermic (Q = -1.85 MeV), this reaction needs nearly 4 MeV proton energy to provide a sufficiently intense neutron yield. Exothermic ^{9}Be(d,n)^{10}B and ^{13}C(d,n)^{14}N (Q = 4.33 MeV and 5.33 MeV respectively) can be utilized at about 1.45 MeV, implying the smallest possible accelerator [16].

For BNCT purposes, all reactions listed in Table 1 require proton/deuteron beams of a few ten mA's in order to produce an intense enough neutron beam. In particular, deuteron induced reactions on ^{9}Be and ^{13}C need at least a 30 mA beam current. In this context a low-energy high-current accelerator is under construction at the Argentine National Atomic Energy Commission to work in conjunction with both targets. The accelerator is a 1.45 MV electro-static quadrupole (ESQ) machine capable of producing 30 mA beams of protons and deuterons of 1.45 MeV [13–14,16].

In this work we present a Monte-Carlo simulation study aimed at optimizing the treatment capabilities for BNCT of the neutron beam produced through the above mentioned accelerator and the ^{13}C(d,n)^{14}N reaction. To epithermalize the primary neutron beam, a Beam Shaping Assembly (BSA) based on an Al + PTFE moderator was simulated with the MCNP code [21]. A Snyder head phantom was placed at the beam port, in order to simulate depth dose profiles in tumor and normal tissues. The optimization study we present here consists in determining the moderator size that maximizes (1) the dose deliverable to tumor and (2) the penetration depth in the phantom, under the constraints imposed by the tolerance doses to normal tissues.

The objective of this work is to evaluate the quality of the above mentioned neutron beam *in terms of dose deliverable to tumor and healthy tissues*. These quantities depend on the characteristics of the neutron beam under free condition. Direct quantities such as the total neutron flux, neutron energy spectrum, gamma ray contamination, directionality of the neutron beam and others, are the so called "free beam parameters" and establish another valid criterion for evaluating whether a neutron beam would be useful for BNCT or not [22]. This criterion is much more restrictive than the one based on doses, since the established values are, in some cases, much more conservative than needed for a useful neutron beam. For this reason, this work is focused on optimizing doses and treatment times, which are the quantities that actually impose a real limitation to a treatment, more than any of the free beam parameters.

1.2. The ^{13}C(d,n)^{14}N reaction

Due to the above mentioned advantages of carbon as a target material, the ^{13}C(d,n)^{14}N is certainly one of the most interesting reactions to produce neutrons through a high current deuteron beam. The lack of residual radioactivity (the residue ^{14}N is stable) makes it possible to avoid any complication related to radioactive waste management of an activated target and/or the implementation of radioisotope traps. Moreover, the low-bombarding energy required (1.45 MeV) allows the utilization of a smaller (and hence, a less complex and cheaper) accelerator.

Because of the large Q-value (Q = 5.33 MeV) the residue ^{14}N can be left – even at low-deuteron energies – in several excited states. For deuterons of 1.45 MeV, the ground and the first eight states are energetically accessible, being the highest at about 6.45 MeV. The neutron spectrum, therefore, has a number of peaks – each of them associated to each of the accessible excites states – going up to about ~6.7 MeV where the neutron peak corresponding to the ground state is located. The relative intensity of each peak is difficult to estimate, unless the partial cross sections associated to each excited state are known for all deuteron energies up to 1.45 MeV.

Colonna et al. measured the neutron spectrum for different emission angles for deuterons of 1.5 MeV [20]. At 0°, 70% of the neutrons are emitted with energies below 1 MeV. These neutrons are mostly associated with the fifth and sixth levels in the ^{14}N residue (at 5.69 and 5.83 MeV). Higher energy peaks from ground to fourth excited states were also observed, coming from the third (4.91 MeV) and the first (2.31 MeV) excited levels mostly. The overall fraction of neutrons with energies higher than 1 MeV is 30%. Most of those neutrons are concentrated in a peak of energy slightly larger than 1 MeV and only 6% of the neutrons emitted with energy greater than 2 MeV. The strong contribution of neutrons below 1 MeV decreases with the emission angle, while an important part of the highest energy neutrons still survives at all angles.

The fact that most of the neutron spectrum at 0° is concentrated below 1 MeV makes this reaction very attractive for BNCT. These neutrons are relatively easy to epithermalize with a moderation process. The presence of higher energy neutrons at large angles could lead in principle to a high fast neutron contamination (something undesired for BNCT) but through a proper beam shaping it does not necessarily result in a worse beam quality, and actually could be advantageous to increase the penetration depth and the total neutron flux at the beam port.

2. Materials and methods

2.1. Beam Shaping Assembly (BSA)

In order to epithermalize the primary neutron spectrum, a Beam Shaping Assembly (BSA) was designed. The BSA is composed

by four nested volumes: the moderator, the neutron reflector, the fast-neutron shield and, gamma shield (Fig. 1). The moderator is a square cross-section volume with a conical-shaped port formed by alternating layers of Al and PTFE of 70 and 125 mm respectively. Within the moderator and after the target, a lead block of 5 cm was added, in order to attenuate gamma rays coming from the de-excitation of the residual nucleus ^{14}N.

The neutron reflector, that delimits the moderator, is made of 15 cm-thick lead walls. Apart from delimiting the beam in the lateral directions, the reflector also acts as a gamma shield for photons produced by neutrons in the BSA materials during the moderation process. In particular, neutron capture in Al, where a prompt gamma ray of 7.72 MeV and a delayed one of 1.78 MeV are produced, is a non-negligible source of undesired gamma radiation.

Surrounding the reflector, there is the fast neutron shield which is a 30 cm thick wall of boronated paraffin (33% paraffin and 67% boric acid H_3BO_3 by weight). In this material, epithermal and fast neutron leakages in the lateral directions are thermalized, and subsequently absorbed in ^{10}B mainly. As a result, gamma rays of 478 keV are emitted in 93% of the boron capture reactions. To attenuate these gamma rays and also those coming from $^{1}H(n,\gamma)$, there is the gamma shield, which is made of 15 cm lead walls.

2.2. BSA optimization

To determine the moderator size, depth dose profiles along a Snyder head phantom were simulated with MCNP [21] for a wide range of BSA cross-sections and lengths. Cross-sections from 20 × 20 to 100 × 100 cm^2 and lengths from 40 to 100 cm were considered. From these profiles, the following quantities were evaluated:

- Treatment time
- Minimum and peak dose delivered to tumor tissues
- Peak dose delivered to healthy tissues (scalp and normal brain)
- Treatable depth, i.e., the maximum depth along the beam line where the radiobiological weighted dose to tumor tissue is higher than 30 Gy-Eq. This value is based on Laramore's model for the minimum dose capable of controlling a malignant glioma [23]

The optimal moderator size was finally determined by the cross-section and length that maximized the minimum and the peak dose to tumor and also the treatable depth.

2.3. Dose and treatment time calculation

The Snyder phantom [24] was sagitally positioned at the beam port. All tissue compositions were taken from ICRU 46 report [25]. We assumed a boron concentration of 15 and 52.5 ppm in normal and tumor brain respectively; and of 22.5 ppm for scalp [26,27]. For skull a conservative value of 15 ppm was assumed [28].

A number of 0.5 cm diameter spheres along the phantom axis (also aligned with the beam) were considered as measurement cells in our simulations (Fig. 1). For the scalp, which has a smaller thickness, a 0.2 cm diameter cell was used.

We shall use hereafter the term "dose" (in Gy-Eq units) to refer to the radiobiological weighted sum given by:

$$D = w_B D_B + w_T D_T + w_F D_F + w_\gamma D_\gamma \quad (1)$$

where D_B, D_T, D_F, D_γ are the four contributions usually considered in BNCT, namely the "boron", "thermal", "fast" and "gamma" absorbed doses respectively [29]. The weighting factors w_i for thermal, gamma and fast doses are the so called Relative Biological Effectiveness' (RBE's). For boron dose the weighting factor is instead called the Compound Biological Effectiveness (CBE) since it not only depends on the radio-sensitivity of the tissue but also on the boron compound and its microdistribution. The RBE's and CBE's factors for the considered biological tissues [26,30] are listed in Table 2.

Depth dose profiles were obtained by simulation of the average neutron and photon fluences (F4 tally) along the Snyder phantom's axis. Through the photon/neutron energy dependent fluence-to-absorbed dose conversion coefficients [31] (implemented with DE and DF cards), each of the D_B, D_T, D_F, D_γ doses were obtained for each measurement cell. Particle weights (WGT cards) were set as the total neutron production (in neutrons/h), in order to obtain the MCNP tally results in Gy/h units. From this, the radiobiological weighted dose rate sum was calculated for each cell, and the treatment time was determined as the maximum time the irradiation could last without exceeding the tolerance limits accepted for healthy brain and scalp. For healthy brain, a peak dose of 11.0 Gy-Eq was adopted [32]. Regarding the scalp, a peak dose of 16.7 Gy-Eq was considered [33]. This value is lower than the usual skin tolerance limit adopted in clinical trials [6], which can go up to 24 Gy-Eq. This choice relies on the fact that the skin tolerance dose decreases as the beam size increases [34]. Due to the shape of the beam port in Fig. 1, a larger skin area would be directly exposed to

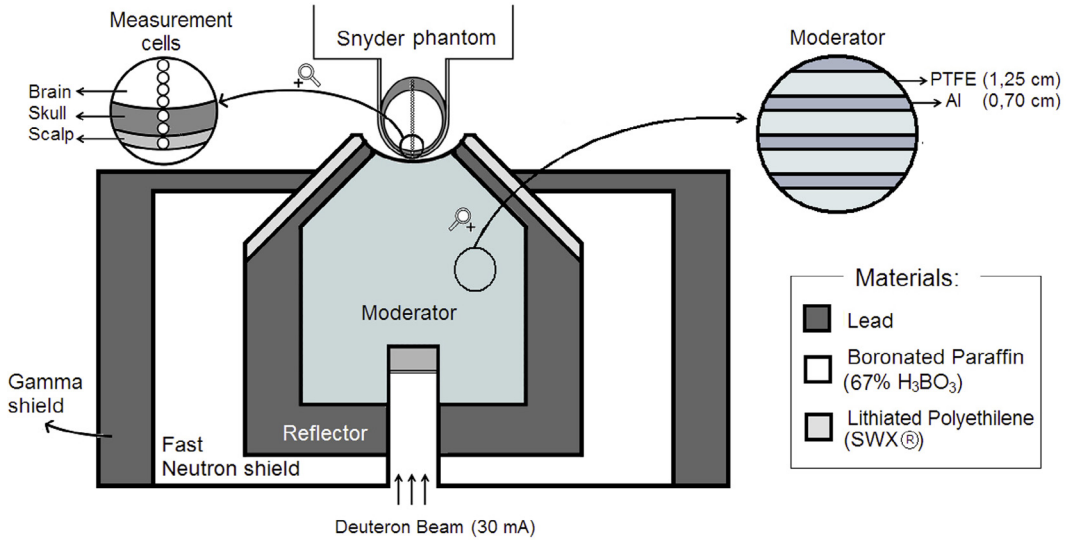

Figure 1. Beam Shaping Assembly design with the Snyder head phantom considered for computational dosimetry.

Table 2
Weighting factors considered for the relevant tissues [26,30].

Weighting Factor	Scalp	Skull	Normal Brain	Tumor
w_B	2.5	1.3	1.3	3.8
w_T	3.2	3.2	3.2	3.2
w_F	3.2	3.2	3.2	3.2
w_γ	1.0	1.0	1.0	1.0

the neutron beam, compared to a flat port of the same diameter. For this reason, a more restrictive tolerance limit was adopted in this work.

2.4. Dose distribution and homogeneity

Tumor dose homogeneity achievable with the optimal BSA was studied. For this purpose, dose volume histograms (DVHs) were calculated for a set of hypothetical brain tumor cases. A tumor of 15.5 cm^3 (i.e., diameter of ~3 cm) was simulated, and the center of the tumor was located at different positions on and off the phantom axis for each case. Two depths were considered: 3.0 cm and 4.5 cm. The first depth corresponds to the point where the thermal neutron flux (and hence, the boron dose) is maximum. The second one corresponds to a deeper position, for which the point of maximum dose falls outside of the tumor volume. For both depths, the tumor was located 1–4 cm off axis.

To calculate DVHs, the whole brain in the Snyder phantom was divided into 13,377 voxels of $0.5 \times 0.5 \times 0.5$ cm^3 each. For each voxel the dose was calculated as described in Section 2.3.

2.5. Free beam parameters

IAEA's beam quality parameters under free conditions [22], namely thermal-to-epithermal neutron flux ratio, fast dose per epithermal neutron (or "fast component") and gamma dose per epithermal neutron (or "gamma component"), were simulated for the optimized BSA. A 2 cm sphere was placed at the beam port axis, where thermal, epithermal, fast neutron, and also photon fluences were simulated. Through fluence-to-dose conversion coefficients, absorbed doses in water were obtained for fast neutrons and gamma rays. Fast and gamma components were calculated then as the ratio between the corresponding dose and the epithermal flux.

3. Results

3.1. BSA optimization

Both the peak and the minimum tumor doses, as well as the treatable depth are maximized when the moderator length is from 65 to 70 cm and the cross-section is from 35×35 cm^2 to 45×45 cm^2. For this set of configurations, the peak tumor dose ranges from 55 to 57 Gy-Eq and the treatable depths are from 5.8 to 6.3 cm. For a tumor of 15.5 cm^3 on the beam axis the minimum tumor dose ranges from 45 to 49 Gy-Eq. Treatment times are from 2 h to 2 h and 20 min.

3.2. Dose performance for the optimized configuration

Fig. 2 shows the depth dose profiles for healthy and tumor tissue obtained for a $65 \times 45 \times 45$ cm^3 moderator. The first two points in the healthy tissue dose profile correspond to the measurement points at scalp and skull respectively. For this BSA configuration, the minimum tumor dose is higher than 45 Gy-Eq for a tumor of about 15.5 cm^3 on the beam axis. This value is quite higher than the minimum dose capable of controlling a malignant glioma established by Laramore. The tumor peak dose and treatable depth are 57 Gy-Eq and 6.2 cm respectively. The peak and mean doses for normal brain are 11.0 Gy-Eq and 4.5 Gy-Eq respectively. For scalp, the peak dose is 14.8 Gy-Eq. The treatment time resulted in 2 h.

Fig. 3 shows depth profiles of dose rate for healthy tissues obtained for each dose contribution. In healthy brain, the boron dose (due to non-specific boron uptake) is the main contribution up to about 5 cm in depth. For scalp (first point in the profile) the boron dose is quite higher than for skull (second point) and also for healthy brain because of the higher boron uptake in this tissue (22.5 ppm for scalp against 15 ppm for skull and brain). Gamma dose, which is the second largest, is mainly due to radiative capture on hydrogen present in biological tissues but also includes all gamma rays produced in the BSA during the moderation process. The hump and valley at the second point for the thermal and fast dose profiles respectively are due to the different composition of the biological tissues. Thermal dose mainly comes from neutron capture on ^{14}N. The mass percentage of this isotope in bone is nearly 50% higher than for healthy brain, and therefore the small hump is observed. Fast dose is mainly due to neutron scattering on ^{1}H. The valley at the second point in the fast dose profile is due to the relatively low concentration of ^{1}H in bone (nearly half the one for scalp and brain).

Concerning dose to scalp, the dominant contribution is the boron dose followed by gamma and fast dose.

3.3. Dose distribution and homogeneity

Table 3 shows the minimum, mean and peak doses delivered to the tumor for each of the cases considered. The minimum and the mean dose to normal brain are also included. DVHs for some representative cases are shown in Fig. 4.

The best performance in terms of dose homogeneity is for a tumor centered on the phantom axis (i.e., along the beam line) at 3 cm in depth, where the thermal neutron flux is maximum. As the center of the tumor is moved off-axis or deeper into the phantom, both the maximum and minimum dose decreases consistently with the reduction of thermal flux in those directions.

3.4. Free beam parameters

Fig. 5 shows the neutron spectrum at the beam port for a $65 \times 45 \times 45$ cm^3 moderator under free beam condition.

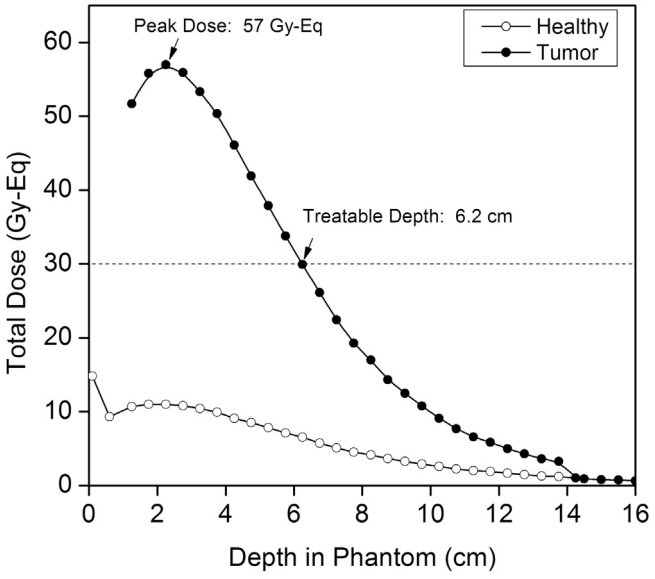

Figure 2. Total healthy tissue and tumor dose profiles for a $65 \times 45 \times 45$ cm^3 moderator. The treatable depth and the peak tumor dose are indicated.

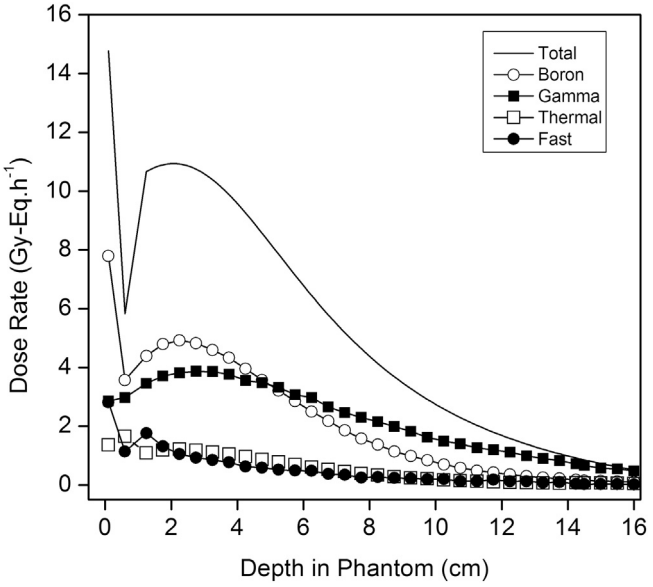

Figure 3. Depth profiles of dose rate components for a $65 \times 45 \times 45$ cm^3 moderator.

To compare, the clinical neutron spectrum from reactor FiR1 in Finland [35,36] was also included. Both spectra were normalized to fit the same scale. Thermal and fast neutrons represent 16% and 7% of the total respectively, while epithermal neutrons are 77%.

IAEA's free beam parameters obtained for the same configuration are listed in Table 4. Fast neutron and gamma components are 4.7×10^{-13} and 7.2×10^{-13} Gy.cm^2 per epithermal neutron respectively, both within the accepted values (2.5 to 13×10^{-13} Gy.cm^2 per epithermal neutron). The thermal-to-epithermal neutron flux ratio is 0.21, which is higher than the recommended value (0.05), but still low enough to not impose a limiting factor from dose to scalp. Regarding this, it should be stressed that the real limitations to a treatment come from the maximum tolerable doses in the different healthy tissues, which are not exceeded with the reaction discussed here. We will address this issue later in the Section 4.

4. Discussion

To assess dose performances obtained here, we shall consider the optimized ^{7}Li(p,n)^{7}Be-based source reported in Ref. [37] (30 mA of 2.3 MeV protons on a ^{7}Li target). The primary spectrum from this neutron source is neutronically superior to the one from ^{13}C(d,n)^{14}N. First, because the primary spectrum is much softer,

Table 3
Minimum, mean and maximum tumor doses obtained for a ~3 cm diameter tumor centered at different points within the Snyder phantom. The minimum, mean and maximum doses to healthy brain are 1.2 Gy-Eq, 4.2 Gy-Eq, and 11.0 Gy-Eq respectively for all cases.

			Tumor Dose (Gy-Eq)		
Depth		Case	Min.	Mean	Max.
3 cm	On axis	#0	45.4	50.1	54.3[a]
	1 cm off-axis	#1	44.3	49.7	54.3
	2 cm off-axis	#2	40.6	48.2	54.1
	3 cm off-axis	#3	35.5	45.5	53.1
	4 cm off-axis	#4	30.1	41.9	50.6
4.5 cm	On axis	#5	39.1	45.7	54.2
	1 cm off-axis	#6	37.7	45.4	54.1
	2 cm off-axis	#7	37.0	44.7	53.1
	3 cm off-axis	#8	35.9	43.3	51.3
	4 cm off-axis	#9	32.9	40.9	49.1

[a] This value is slightly lower than the one in Fig. 2 because the volume of the voxels are larger that the volume of the measurement cells considered for the dose profiles.

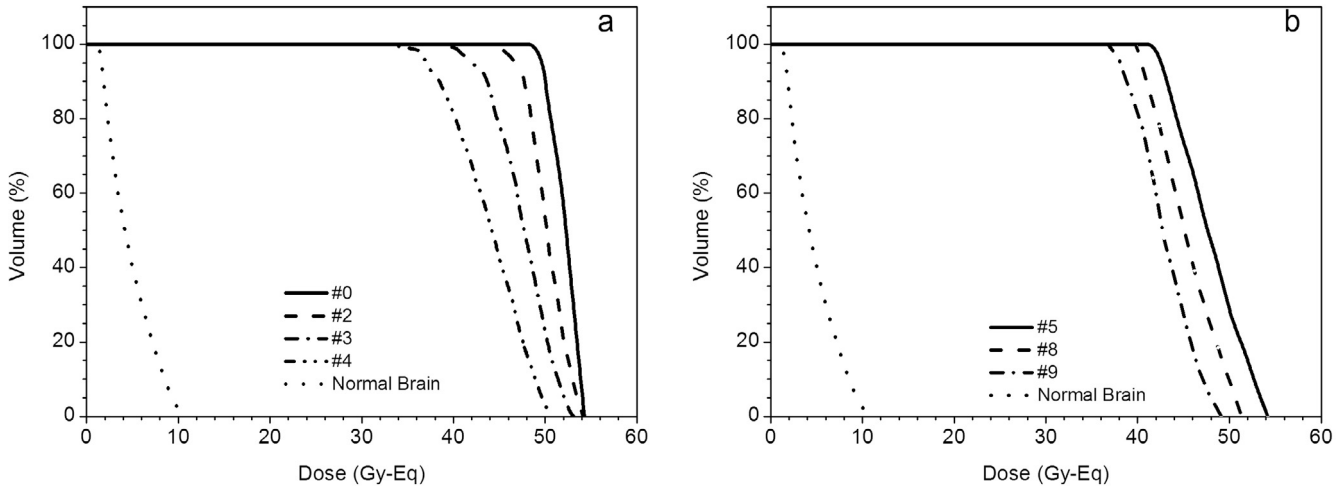

Figure 4. Dose Volume Histograms (DVH) for tumor and healthy brain. (a) A 15.5 cm^3 tumor centered at a depth of 3 cm: case #0 = on beam axis, case #2, #3 and #4 = 2, 3 and 4 cm off-axis respectively. (b) The same tumor centered at a depth of 4.5 cm: case #5 = on beam axis, case #8 and #9 = 3 and 4 cm off axis respectively.

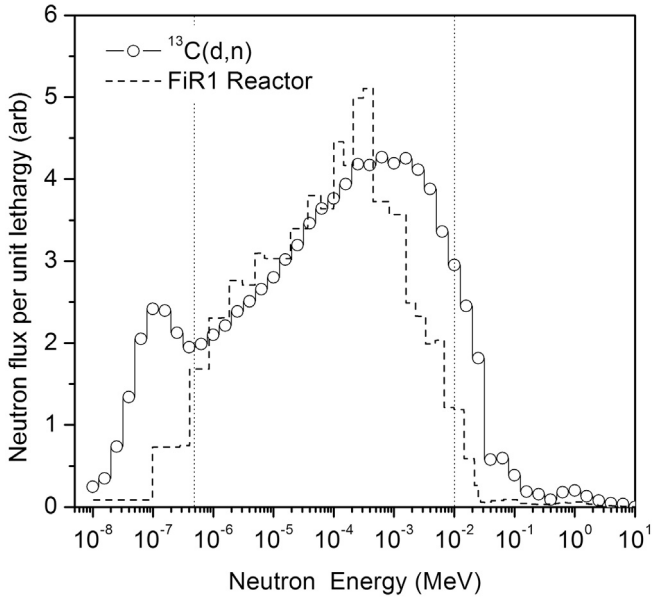

Figure 5. Free beam neutron spectrum at the beam port for a 65 × 45 × 45 cm^3 moderator. Reactor FiR1 clinical neutron spectrum [35] is shown in dashed line. The dotted vertical lines indicate the usual division into thermal (<0.5 eV), epithermal (0.5 eV–10 keV) and fast (>10 keV) energies.

with neutron energies <600 keV; and second, because the neutron yield is significantly higher (5.8×10^{11} against 1.9×10^{11} neutrons/mC). Despite the neutronic advantages of the ^{7}Li(p,n) over ^{13}C(d,n), dose performances are comparable, as shown in Table 5.

In Ref. [37] the authors define the treatable depth as the maximum depth for which the Tumor Control Probability (TCP) for a tumor of 1 cm^3 is 98%. This TCP corresponds to a tumor dose of 38 Gy-Eq. To simplify the comparison we include in Table 5 the parameter "Depth $D_{98\%}$" which is the treatable depth as defined in Ref [37]. This is just another alternative to the definition given above in Section 2, using Laramore's model.

The main difference between both neutron sources is in treatment time, being of only 1 h for the ^{7}Li case, consistently with the fact that the neutron yield for this source is more than twice the one from ^{13}C(d,n)^{14}N.

For the ^{13}C(d,n) source, the treatment time resulted in 2 h, which is probably too long for a single scheme treatment. There is, though, no impediment to split the treatment into two sessions; it was actually practiced in clinical work [38] and it may be advantageous from a biological point of view [39]. Another approach is to increase the deuteron beam intensity, something which by no means is out of reach of present technology.

It is important to mention that limiting the treatment time to 1 h is possible by using a smaller moderator (55 × 45 × 45 cm^3). In this case, peak doses to tumor, normal brain and scalp are 50 Gy-Eq, 11.0 Gy-Eq and 15.7 Gy-Eq respectively. Dose performances would no longer be optimized, but would still be acceptable.

Dose component analysis in 3.2 showed that the boron dose (due to non-specific uptake) is the largest one, both for scalp and healthy brain. This is consistent with the fact that a thermal contamination is present in the neutron spectrum at the beam port (Fig. 5). This thermal component can be reduced by adding a thin layer of lithium carbonate enriched in ^{6}Li at the beam port. Table 6 shows the results obtained for a 1 mm and a 2 mm layer added to the optimal configuration (65 × 45 × 45 cm^3 moderator) respectively.

The thermal to epithermal flux ratio is significantly reduced. As a consequence, the dose to scalp is reduced in about 20% and the depth $D_{98\%}$ is slightly increased, reaching comparable values (or even better) than the ones for the Li target. Moreover, with a 2 mm layer, the thermal-to-epithermal neutron flux ratio becomes comparable to the one at FiR1 clinical beam. These results suggest that the beam quality can probably still be improved through further BSA optimization which is planned for future work.

Dose performance for a ^{7}Li(p,n)–based neutron source was reported by Herrera et al. [40], where treatment plans for a group of patients diagnosed with glioblastoma multiforme (GBM) were optimized. There too, a tumor dose lower limit of 30 Gy-Eq is adopted, based on Laramore's model and on clinical results reported by Yamamoto et al. [41]. Concerning dose to healthy brain, a mean whole brain dose between 5 and 7 Gy-Eq was associated to 50% of somnolence in different clinical experiences [32,41,42].

Table 4
Free beam parameters for the optimal configuration (65 × 45 × 45 cm^3 moderator). The corresponding values reported for reactor Fir1 clinical beam [35] are also included when available (in brackets).

Parameter		Value	Recommended Value [22]:
Fast neutron component:	D_F/ψ_E	4.7×10^{-13} Gy.cm^2/epithermal neutron [1.4×10^{-13}]	$2.5–13 \times 10^{-13}$ Gy.cm^2/epithermal neutron
Gamma ray component:	D_γ/ψ_E	7.2×10^{-13} Gy.cm^2/epithermal neutron	$2.5–13 \times 10^{-13}$ Gy.cm^2/epithermal neutron
Thermal-to-Epithermal neutron flux ratio:	φ_T/φ_E	0.21 [0.06]	0.05

ψ_E = Epithermal neutron fluence.
φ_E = Epithermal neutron flux.
φ_T = Thermal neutron flux.

Table 5
Dose performance comparison between a ^{13}C(d,n)^{14}N-based neutron source and a ^{7}Li(p,n)^{7}Be-based one.

	Peak Dose [Gy-Eq]			Depth	Treatment
	BT[a]	NB[b]	S[c]	$D_{98\%}$ [d]	Time
^{13}C(d,n)^{14}N (1.45 MeV, 30 mA)	57.0	11.0	14.8	5.2 cm	2 h
^{7}Li(p,n)^{7}Be (2.3 MeV, 30 mA) [37]	56.7	11.0	12.4	5.4 cm	1 h

[a] BT: Brain tumor.
[b] NB: Normal Brain.
[c] S: Scalp.
[d] $D_{98\%}$: Maximum depth along the beam axis for which the Tumor Control Probability (TCP) is higher than 98% for a tumor of 1 cm^3.

Table 6
Free beam parameters and dose performances obtained for the optimal configuration (65 × 45 × 45 cm^3 moderator) when a 1 mm and a 2 mm layer of Li_2CO_3 (95% ^6Li) is added at the beam port.

		1 mm	2 mm	Without Li_2CO_3
Thermal-to-epithermal neutron flux ratio:		0.11	0.07	0.20
Epithermal flux[a]: [n_{epi}/cm^2-s]		2.1×10^8	2.0×10^8	2.2×10^8
Peak Doses:	Tumor	57.4	56.2	57.0
[Gy-Eq]	Scalp	11.8	11.8	14.8
	Normal Brain	11.0	11.0	11.0
Depth $D_{98\%}$[b]	[cm]	5.5	5.6	5.2
Treatment time		2 h 20 m	2 h 30 m	2 h

[a] Relative uncertainties are 0.1%.
[b] Absolute uncertainties are 0.05 cm.

Results in 3.3 show that it is possible to deliver more than 30 Gy-Eq to a relatively large tumor (3 cm diameter) located either on or off axis. A whole brain mean dose lower than 5 Gy-Eq was obtained for all evaluated cases. These results suggest that dose performances comparable to those reported in clinical work may be obtained through proper beam optimization based on a treatment planning system.

5. Conclusions

The $^{13}C(d,n)^{14}N$ reaction was evaluated as an epithermal neutron source for Accelerator-Based Boron Neutron Capture Therapy. Through a 30 mA beam of deuterons of 1.45 MeV this reaction can produce a sufficiently intense neutron beam to deliver a significant dose to tumor tissue up to 6.2 cm in depth. A peak dose of 57 Gy-Eq is feasible in a fractionated scheme of two sessions of 1 h each, while keeping all the doses to healthy tissues below the tolerance limits. With the exception of treatment time, dose performances achieved here are comparable to those obtained through the optimal $^7Li(p,n)^7Be$ reaction, something which can be compensated by increasing the deuteron beam intensity.

Finally, it is important to emphasize the advantages that a ^{13}C (d,n) – based neutron source would imply. In addition to the suitable thermomechanical properties of ^{13}C as a target, this reaction does not produce residual radioactivity, which means a significant advantage for the aim of implementing BNCT in a hospital environment. Last but not least, the low deuteron energy required (1.45 MeV) compared to other neutron producing reactions, implies the smallest possible, and hence, less costly, accelerator for BNCT.

References

[1] Kankaanranta L, Seppälä T, Koivunoro H, Saarilahti K, Atula T, Collan J, et al. Boron neutron capture therapy in the treatment of locally recurred head-and-neck cancer: final analysis of a phase I/II trial. Int J Radiat Oncol Biol Phys 2012;82:e67–75.
[2] Yamamoto T, Matsumura A, Nakai K, Shibata Y, Endo K, Sakurai F, et al. Current clinical results of the Tsukuba BNCT trial. Appl Radiat Isot 2004;61:1089–93.
[3] Kageji T, Mizobuchi Y, Nagahiro S, Nakagawa Y, Kumada H. Clinical results of boron neutron capture therapy (BNCT) for glioblastoma. Appl Radiat Isot 2011;69:1823–5.
[4] Miyatake S, Tamura Y, Kawabata S, Iida K, Kuroiwa T, Ono K. Boron neutron capture therapy for malignant tumors related to meningiomas. Neurosurgery 2007;61:82–90.
[5] Wang LW, Wang SJ, Chu PY, Ho CY, Jiang SH, Liu YH, et al. BNCT for locally recurrent head and neck cancer: preliminary clinical experience for a phase I/II trial at Tsin Hua Open-Pool Reactor. Appl Radiat Isot 2011;69:1803–6.
[6] Menéndez PR, Roth BM, Pereira DM, Casal MR, González SJ, Feld DB, et al. BNCT for skin melanoma in extremities: updated Argentine clinical results. Appl Radiat Isot 2009;67:s50–3.
[7] Yoshioka M, Kurihara T, Kurokawa S, Kobayashi H, Matsumoto H, Matsumoto N, et al. Construction of an accelerator-based BNCT facility at the Ibaraki Neutron Medical Research Center. In: Proceedings of LINAC 2014, Geneva, Switzerland; p. 230–32.
[8] Halfon S, Paul M, Arenshtam A, Berkovits D, Bisyakoev M, Eliyahu I, et al. High-power liquid-lithium target prototype for accelerator-based boron neutron capture therapy. Appl Radiat Isot 2011;69:1654–6.
[9] Aleynik V, Burdakov A, Davydenko V, Ivanov A, Kanygin V, Kuznetsov A, et al. BINP accelerator based epithermal neutron source. Appl Radiat Isot 2011;69:1635–8.
[10] Kononov OE, Kononov VN, Bokhovko MV, Korobeynikov VV, Soloviev AN, Sysoev AS, et al. Optimization of an accelerator-based epithermal neutron source for neutron capture therapy. Appl Radiat Isot 2004;61:1009–13.
[11] Pisent A, Colautti P, Esposito J, De Nardo L, Conte V, Agosteo D, et al. Progress on the accelerator based SPES-BNCT project at INFN Legnaro. J Phys Conf Ser 2006;41:391–9.
[12] Culbertson CN, Green S, Mason AJ, Picton D, Baugh G, Hugtenburg RP, et al. In-phantom characterisation studies at the Birmingham Accelerator Generated epIthermal Neutron Source (BAGINS) BNCT facility. Appl Radiat Isot 2004;61:733–8.
[13] Kreiner AJ, Castell W, Baldo M, et al. Development of a Tandem-Electrostatic-Quadrupole facility for Accelerator-Based Boron Neutron Capture Therapy. Appl Radiat Isot 2011;69:1672–5.
[14] Kreiner AJ, Baldo M, Bergueiro J, et al. Accelerator-based BNCT. Appl Radiat Isot 2014;88:185–9. and references therein.
[15] Jung Joo-Young, Bo Lu, Yoon Do-Kun, Hong Key Jo, Jang HongSeok, Liu Chihray, et al. Therapy region monitoring based on PET using 478 keV single prompt gamma ray during BNCT: a Monte Carlo simulation study. Phys Med 2016;32 (4):562–7.
[16] Kreiner AJ, Bergueiro J, Cartelli D, Baldo M, Castell W, Gomez Asoia J, et al. Present status of accelerator-based BNCT. Rep Pract Oncol Radiother 2016;21:95–101. and reference therein.
[17] Lee CL, Zhou XL. Thick target neutron yields for the $^7Li(p,n)^7Be$ reaction near threshold. Nucl Instrum Methods Phys Res Sect B 1999;152:1–11. doi: http://dx.doi.org/10.1016/S0168-583X(99)00026-9.
[18] Howard WB, Grimes SM, Massey TN, Al-Quraishi SI, Jacobs DK, et al. Measurement of the thick target $^9Be(p,n)$ neutron energy spectra. Nucl Sci Eng 2001;138:145–60.
[19] Capoulat ME, Minsky DM, Kreiner AJ. Computational assessment of deep-seated tumor treatment capability of the $^9Be(d,n)^{10}B$ reaction for accelerator-based boron neutron capture therapy. Phys Med 2014;30:133–46.
[20] Colonna N, Beaulieu L, Phair L, Wozniak GJ, Moretto LG, Chu WT, Ludewigt BA. Measurements of low-energy (d, n) reactions for BNCT. Med Phys 1999;26:793–8.
[21] Brown F, et al. MCNP Version 5. Tech Rep LA-UR-02-3935. Los Alamos National Laboratory Reports, 2002.
[22] IAEA TEC-DOC 1223. Current Status of Neutron Capture Therapy. IAEA Publications. International Atomic Energy Agency; 2001.
[23] Laramore GE, Wheeler FJ, Wessol DE, Selzer KJ, Griffin TW. A tumor control curve for malignant gliomas derived from fast neutron radiotherapy data: implications for treatment delivery and compound selection. In: Larson B, editor. Proceedings of the 7th International Symposium on Neutron Capture Therapy for Cancer. New York: Elsevier Science; 1997. p. 580–7.
[24] Goorley JT, Kiger III WS, Zamenhof RG. Reference dosimetry calculations for Neutron Capture Therapy with comparison of analytical and voxel models. Med Phys 2002;29:145–56.
[25] ICRU 46. Photon, Electron, Proton and Neutron Interaction Data for Body Tissues Tech. Rep.. International Commission on Radiation Units and Measurements; 1992.
[26] Kankaanranta L, Seppälä T, Koivunoro H, Saarilahti K, Atula T, Collan J, et al. Boron neutron capture therapy in the treatment of locally recurred head-and-neck cancer: final analysis of a phase I/II trial. Int J Radiat Oncol Biol Phys 2007;69:475–82.
[27] Yamamoto T, Nakai K, Matsumura A. Boron neutron capture therapy for glioblastoma. Cancer Lett 2008;262:143–52.
[28] Ferrari C, Zonta C, Cansolino L, et al. Selective uptake of p-boronophenylalanine by osteosarcoma cells for boron neutron capture therapy. Appl Radiat Isot 2009;67:S341–4.
[29] Savolainen S, Auterinen I, Aschan C, Hiismäki P, Kortesniemi M, Kosunen A, et al. Dosimetry chain for the treatments of glioma patients in the epithermal neutron beam at the Finnish BNCT Facility (FiR1). Med Biol Eng Comput 1999;34:388–9.
[30] Joensuu H, Kankaanranta L, Seppälä T, Auterinen I, Kallio M, Kulvik M, et al. Boron neutron capture therapy of brain tumors: clinical trials at the Finnish facility using boronophenylalanine. J Neurooncol 2003;62:123–34.

[31] Chadwick MB, Barschall HH, Caswell RS, DeLuca PM, Hale GM, Jones DT. A consistent set of neutron kerma coefficients from thermal to 150 MeV for biologically important materials. Med Phys 1999;26:974–91.
[32] Coderre JA, Hopewell JW, Turcotte JC, Riley KJ, Binns PJ, Kiger III WS, et al. Tolerance of normal human brain to boron neutron capture therapy. Appl Radiat Isot 2004;61:1083–7.
[33] Blaumann HR, González SJ, Longhino J, Santa Cruz GA, Calzetta Larrieu OA, Bonomi MR, et al. Boron neutron capture therapy of skin melanomas at the RA-6 reactor: a procedural approach to beam set up and performance evaluation for upcoming clinical trials. Med Phys 2004;31:70–80.
[34] Douglas BG. Implications of the cuadratic cell survival curve and human skin radiation 'tolerance dose' on fractionation and superfractionation dose selection. Int J Radiat Oncol Biol Phys 1982;8:1135–42.
[35] Auterinen I, Serén T, Anttila K, Kosunen A, Savolainen S. Measurement of free beam neutron spectra at eight BNCT facilities worldwide. Appl Radiat Isot 2004;61:1021–6.
[36] Savolainen S, Kortesniemi M, Timonen M, Reijonen V, Kuusela L, Uusi-Simola J, et al. Boron Neutron Capture Therapy (BNCT) in Finland: technological and physical prospects after 20 years of experiences. Phys Med 2013;29 (3):233–48.
[37] Minsky DM, Kreiner AJ. Beam shaping assembly optimization for ^{7}Li(p, n)^{7}Be accelerator based BNCT. Appl Radiat Isot 2014;88:233–7.
[38] Wang Ling-Wei, Chen Yi-Wei, Ho Ching-Yin, Hsueh Liu Yen-Wan, Chou Fong-In, Liu Yuan-Hao, et al. Fractionated BNCT for locally recurrent head and neck cancer: experience from a phase I/II clinical trial at Tsing Hua Open-Pool Reactor. Appl Radiat Isot 2014;88:23–7.
[39] Molinari AJ, Pozzi EC, Monti Hughes A, Heber EM, Garabalino MA, Thorp SI, et al. "Sequential" boron neutron capture therapy (BNCT): a novel approach to BNCT for the treatment of oral cancer in the hamster cheek pouch model. Radiat Res 2001;175:463–72.
[40] Herrera MS, González SJ, Minsky DM, Kreiner AJ. Evaluation of performance of an accelerator-based BNCT facility for the treatment of different tumor targets. Phys Med 2013;29:436–46.
[41] Yamamoto T, Nakai K, Kageji T, Kumada H, Endo K, Matsuda M, et al. Boron neutron capture therapy for newly diagnosed glioblastoma. Radiother Oncol 2009;91:81–4.
[42] Riley KJ, Binns PJ, Harling OK, Albritton JR, Kiger III WS, Rezaei A, et al. An international dosimetry exchange for BNCT Part II: computational dosimetry normalizations. Med Phys 2008;35:5419–25.